AD-A042 182 NAVAL SURFACE WEAPONS CENTER WHITE OAK LAB SILVER SP--ETC F/G 10/3
MEASUREMENT OF BATTERY SEPARATOR RESISTANCES IN LOW IMPEDANCE C--ETC(U)
APR 77 W P KILROY, C T MOYNIHAN

UNCLASSIFIED NSWC/WOL/TR-77-47 NL

| OF |
AD
A042182

END

DATE
FILMED
8-77

NSWC/WOL/TR 77-47

12 D.S.

NSWC/WOL/TR 77-47

NSWC TECHNICAL REPORT

WHITE OAK LABORATORY

MEASUREMENT OF BATTERY SEPARATOR RESISTANCES IN LOW IMPEDANCE CONDUCTIVITY BY A. C. BRIDGE TECHNIQUES

BY
W.P. Kilroy
C.T. Moynihan

26 APRIL 1977

NAVAL SURFACE WEAPONS CENTER
WHITE OAK LABORATORY
SILVER SPRING, MARYLAND 20910

- Approved for public release; distribution unlimited.

NAVAL SURFACE WEAPONS CENTER
WHITE OAK, SILVER SPRING, MARYLAND 20910

UNCLASSIFIED

SECURITY CLASSIFICATION OF THIS PAGE *(When Data Entered)*

REPORT DOCUMENTATION PAGE		READ INSTRUCTIONS BEFORE COMPLETING FORM
1. REPORT NUMBER NSWC/WOL/TR-77-47	2. GOVT ACCESSION NO.	3. RECIPIENT'S CATALOG NUMBER
4. TITLE *(and Subtitle)* Measurement of Battery Separator Resistances in Low Impedance Conductivity Cells by A.C.Bridge Techniques.		5. TYPE OF REPORT & PERIOD COVERED Progress rept., 6. PERFORMING ORG. REPORT NUMBER
7. AUTHOR(s) W. P. Kilroy and C. T. Moynihan		8. CONTRACT OR GRANT NUMBER(s)
9. PERFORMING ORGANIZATION NAME AND ADDRESS Naval Surface Weapons Center White Oak Laboratory White Oak, Silver Spring, Maryland 20910		10. PROGRAM ELEMENT, PROJECT, TASK AREA & WORK UNIT NUMBERS 62543N; F43431 SF43431302 WR33BB;
11. CONTROLLING OFFICE NAME AND ADDRESS 18p.		12. REPORT DATE 26 April 1977 13. NUMBER OF PAGES 16
14. MONITORING AGENCY NAME & ADDRESS *(if different from Controlling Office)*		15. SECURITY CLASS. *(of this report)* Unclassified 15a. DECLASSIFICATION/DOWNGRADING SCHEDULE

16. DISTRIBUTION STATEMENT *(of this Report)*

Approved for public release; distribution unlimited

17. DISTRIBUTION STATEMENT *(of the abstract entered in Block 20, if different from Report)*

18. SUPPLEMENTARY NOTES

19. KEY WORDS *(Continue on reverse side if necessary and identify by block number)*

Capacitance; resistance; battery separator

20. ABSTRACT *(Continue on reverse side if necessary and identify by block number)*

Measurement of the resistance of battery separator membranes is frequently accomplished by taking the difference between the resistances of an electrolyte filled conductivity cell with and without the separator inserted between the electrodes. For low resistance separators this may involve measurements of impedances of a few tenths of an ohm. It is shown via equibalent circuit analysis and experimental data on a low impedance cell filled with 45% aqueous KOH solution that ac bridge measurements of separator resistances can be seriously in error if proper account is not taken of electrode impedance.

DD FORM 1 JAN 73 1473 EDITION OF 1 NOV 65 IS OBSOLETE
S/N 0102-014-6601

UNCLASSIFIED

SECURITY CLASSIFICATION OF THIS PAGE *(When Data Entered)*

391 596

LB

NSWC/WOL/TR 77-47 26 April 1977

MEASUREMENT OF BATTERY SEPARATOR RESISTANCES IN LOW IMPEDANCE CONDUCTIVITY CELLS BY A. C. BRIDGE TECHNIQUES

A new separator material for alkaline batteries is presently under development. One of the criteria that membranes made from this material must meet is a low electrical resistance. Since resistance measurements are used during development to accept or reject a material, it is important that the technique used yield accurate values.

This investigation was undertaken to determine the reliability of measuring very low separator resistances ($\leq 0.01\Omega$) in low impedance conductivity cells.

J. R. DIXON
By direction

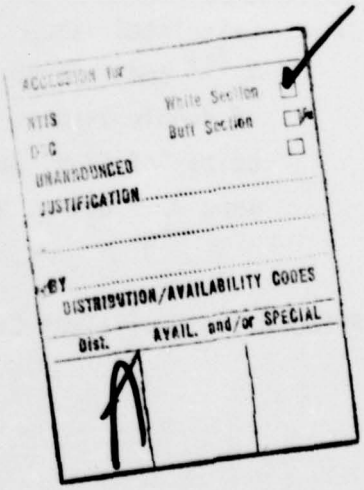

TABLE OF CONTENTS

ILLUSTRATIONS

TABLES

INTRODUCTION

In order to increase the electrochemical efficiency, batteries are designed to have a low internal resistance. The major contributors to the internal resistance of a battery are the electrolyte and the separator. The separator is usually a membrane permeable to the electrolyte ions and is used to prevent direct mixing of the anolyte and catholyte. Efforts to improve battery performance are often centered on the development of a stable separator which contributes relatively little to the internal resistance, ideally, a small fraction of the electrolyte resistance.

Assessment of the contribution of a separator material to the battery internal resistance is typically made[1] first by measuring the resistance of the electrolyte solution, R_{sol}, between two plane parallel electrodes in a conductivity cell. After this the separator is inserted between the two electrodes in the electrolyte filled cell and the new resistance, $(R_{sol} + R_{sep})$, measured. The contribution of separator to the internal resistance, R_{sep}, is then the difference between the two resistance measurements. Plainly an accurate measurement of R_{sep} requires that R_{sep} not be negligible compared to R_{sol}, i.e., R_{sep} must contribute an accurately measurable increment to R_{sol}.

A case in point for the present paper is a separator for silver-zinc batteries using 30-45% KOH solution as electrolyte in which a good separator material may contribute as little as 15.5 Ω/m^2 (0.01 Ω/in^2) to the internal resistance. An accurate measurement of R_{sep} thus requires that R_{sol} be of the order of 155 Ω/m^2 (0.1 Ω/in^2) or smaller.

The usual method of carrying out resistance measurements of this type is by means of a conventional ac Wheatstone bridge at audio frequencies. The cell impedance is balanced against a parallel resistance-capacitance combination (R_p, C_p) as shown in Fig. 1. The balancing resistance R_p is usually identified

---

1. A.J.Salkind and J.J.Kelley, in "Characteristics of Separators for Alkaline Silver Oxide Zinc Secondary Batteries--Screening Methods", J.E.Cooper and A.Fleisher, Eds., Air Force Aero Propulsion Laboratory, WPAFB, Ohio, 1964, pg 69-75.

with the cell resistance, R_{sol} or $(R_{sep} + R_{sol})$. As has been pointed out numerous times in the literature[2], the equivalent ac circuit of the cell is not a parallel resistance-capacitance combination, i.e., it does not correspond to the balancing circuit configuration, R_p in parallel with C_p. This in turn can lead to large errors in the measurement of R_{sol} and $(R_{sep} + R_{sol})$, as shown below.

The simplest approximations[2] to the true equivalent circuits of a low impedance conductivity cell containing electrolyte and electrolyte plus separator are shown respectively in Figs. 2a and 2b. R_L is the resistance of the leads between the bridge and conductivity cell, and C_{dl} represents the double layer capacitances at the electrode surfaces. Hence the true first approximation of the equivalent circuit of the cell has the resistive elements (R_L, R_{sol}, and R_{sep}) in series with a capacitance, C_{dl}.

For Fig. 2a, the complex impedance is

$$Z^{(a)} = (R_L + R_{sol}) + 1/i\omega C_{dl} \tag{1}$$

where $\omega = 2\pi f$ is the angular frequency. If the circuit of Fig. 2a were measured on the bridge of Fig. 1, the equivalent parallel resistance would be

$$R_p^{(a)} = \frac{1}{\mathrm{Re}(1/Z^{(a)})} = \frac{(R_L + R_{sol})^2 + (1/\omega C_{dl})^2}{R_L + R_{sol}} \tag{2}$$

where Re designates the real part of the complex number. Similarly the complex impedance of the circuit of Fig. 2b is

$$Z^{(b)} = (R_L + R_{sol} + R_{sep}) + 1/i\omega C_{dl} \tag{3}$$

and the equivalent parallel resistance is

$$R_p^{(b)} = \frac{1}{\mathrm{Re}(1/Z^{(b)})} = \frac{(R_L + R_{sol} + R_{sep})^2 + (1/\omega C_{dl})^2}{R_L + R_{sol} + R_{sep}} \tag{4}$$

In the usual procedure for determination of the separator resistance using a

2. J. Braunstein and G. D. Robbins, J. Chem. Educ., 48, 52 (1971)

bridge like that of Fig. 1, the apparent separator resistance would be taken to be

$$R_{sep,app.} = R_p^{(b)} - R_p^{(a)} = R_{sep}\left[1 - \frac{1}{(R_L+R_{sol}+R_{sep})(R_L+R_{sol})(1/\omega C_{dl})^2}\right] \quad (5)$$

In Table 1, we show the results of calculations via Eqs. (2), (4), and (5) of the apparent electrolyte plus lead resistance $R_p^{(a)}$ and the apparent separator resistance $R_{sep,app.}$ as a function of C_{dl} and frequency in the audio range. We have used values of R_L, R_{sol}, and R_{sep} typical for low resistance separator membranes in a highly conducting electrolyte such as 45% aqueous KOH solution. Clearly $R_p^{(a)}$ approaches the actual value, 0.2 Ω, of $(R_L + R_{sol})$ and $R_{sep,app.}$ approaches the actual value, 0.01 Ω, of R_{sep} only in the limits of high frequency and/or high double layer capacitance.

At present it is not known to what degree these limiting conditions have been satisfied in actual measurements of separator resistances. Indeed, it is similarly unknown to what degree the simple circuits of Fig. 2 are a sufficiently accurate representation of the cell for obtaining an accurate determination of R_{sep} by measuring the equivalent series resistance of the cell. We do note, however, from Table 1 that a correct determination of $(R_L + R_{sol})$ guarantees a correct determination of R_{sep}. Consequently, in the present study we have carried out a series of resistance and capacitance measurements at various frequencies in order to determine what errors, if any, may arise in these determinations. The measurements were made on a cell used in measurements of separator resistances and filled with 45% KOH.

TABLE 1 Calculated values of apparent electrolyte plus lead resistance $R_p^{(a)}$ and apparent separator resistance $R_{sep,app.}$ as a function of double layer capacitance C_{dl} and frequency f for the circuits of Figs. 2a and 2b. Assumed values of the other components were

$R_L = 0.1\ \Omega$

$R_{sol} = 0.1\ \Omega$

$R_{sep} = 0.01\ \Omega$

	$f = 10^2$ Hz		$f = 10^3$ Hz		$f = 10^4$ Hz	
$C_{dl}(\mu F)$	$R_p^{(a)}(\Omega)$	$R_{sep,app}(\Omega)$	$R_p^{(a)}(\Omega)$	$R_{sep,app}(\Omega)$	$R_p^{(a)}(\Omega)$	$R_{sep,app}(\Omega)$
10	12.7×10^4	-6.03×10^3	12.7×10^2	-6.03×10^1	12.9	-0.593
10^2	12.7×10^2	-6.03×10^1	12.9	-0.593	0.327	0.0040
10^3	12.9	-0.593	0.327	0.0040	0.201	0.0099
10^4	0.327	0.0040	0.201	0.0099	0.200	0.0100
10^5	0.201	0.0099	0.200	0.0100	0.200	0.0100

EXPERIMENTAL SECTION

The conductivity cell used in these experiments was obtained from RAI Research Corporation and is shown in Fig. 3. It consists of two heavy gauge square Pt electrodes, 2.54 cm on a side mounted plane parallel and 0.25 cm apart in a lucite holder. The cell can be disassembled and the electrodes removed. The cell also contains a provision for inserting a separator film between the two electrodes. This feature was not used in the present study.

In order to assess the effect of electrode double layer capacitance, measurements were carried out for two electrode conditions: bright, polished platinum electrodes (unplatinized) and electrodes coated electrolytically with a heavy deposit of platinum black (platinized). The fine granular Pt black deposit cause[s] large increase in the electrode surface area, leading to an increase in [double] layer capacitance.

[The] assembled cell was filled with Fisher Scientific 45 wt % aqueous KOH solution and allowed to stand overnight, refilled with fresh solution and the equivalent parallel resistance and capacitance, R_p and C_p, measured at 25.0 $\pm$ 0.1°C over the frequency range 50 to 5000 Hz. Resistance measurements (accuracy 1%) were made using a General Radio 1650B impedance bridge. An external capacitance balancing decade box adjustable in steps of 10^{-4} μF was connected via shielded cables in parallel with the balancing resistance slide wire in the bridge. Current (ac) was supplied by a Hewlett Packard 200 CD Oscillator; frequency was measured with an Anadex CF 500R counter.

A similar set of measurements of R_p and C_p were made at 25°C with the conductivity cell with platinized electrodes filled with 0.01 M KCl aqueous solution in order to obtain the calibration constant for the cell. To obtain the resistance of the leads to the cell, R_L, the cell was filled with mercury to short circuit the two electrodes and the resistance measured; this gave a value of R_L = 0.173 Ω.

A capillary conductivity cell with platinized platinum electrodes whose cell constant (22.3 cm^{-1}) had been determined previously by calibration with 0.01 M KCl solution was used to measure the conductivity of the 45% KOH solution. The equivalent parallel resistance of this cell filled with the KOH solution was 47.9 Ω at 25.0°C and 1 kHz.

RESULTS AND DISCUSSION

The resistance, R_p, of the cell filled with 0.01 M KCl solution was 27.5 $\pm$ 0.1 Ω and independent of frequency over the entire frequency range. This indicates (cf. Eq. (2)) that contributions to R_p from frequency dependent electrode impedance terms such as $(1/\omega C_{dl})$ are negligible compared to the contribution from the $(R_L + R_{sol})$ term, so that $(R_L + R_{sol})$ may be taken as the measured R_p value of 27.5 Ω. Subtracting the measured value of R_L from this gives R_{sol} = 27.3 Ω. The cell calibration constant, (L/A), may then be calculated from

$$K_{sol} = (L/A)/R_{sol} \tag{6}$$

where K_{sol} is the conductivity of the electrolyte solution. Using K_{sol} = 0.0014127 $\Omega^{-1}cm^{-1}$ for 0.01 M KCl solution at 25°C,[3] the cell constant (L/A) is 0.0386cm^{-1}. This is in good agreement with the less precise (L/A) value of 0.039cm^{-1} calculated from the electrode area ($A = (2.54cm)^2$) and electrode separation (L = 0.25cm).

Similarly the resistance R_p of the 45% KOH solution in the capillary conductivity cell is sufficiently large that it may be used directly to calculate the conductivity of this solution. This gives 0.465 $\Omega^{-1}cm^{-1}$ for K_{sol} of the 45% KOH solution at 25°C.

In Figs. 4 and 5 the bridge measurements of R_p and C_p respectively are plotted versus frequency for the 45% KOH solution in the conductivity cell with unplatinized and platinized electrodes. Also plotted are the equivalent series resistance R_s and capacitance C_s calculated from the complex admittance

$$Y = \frac{1}{R_p} + i\omega C_p \tag{7}$$

via the equations

$$R_s = \mathrm{Re}(1/Y) = \frac{R_p}{1 + (\omega R_p C_p)^2} \tag{8}$$

---

3. R. A. Robinson and R. H. Stokes, "Electrolyte Solutions", Butterworths, London, 1965, p. 466.

$$C_s = -\frac{1}{\omega\ \mathrm{Im}(1/Y)} = C_p\left[1 + \frac{1}{(\omega R_p C_p)^2}\right] \tag{9}$$

where Re and Im designate the real and imaginary parts respectively.

If the circuit of Fig. 2a were an accurate representation of the cell equivalent circuit, R_s and C_s would be frequency independent and equal resprectively to $(R_L + R_{sol})$ and C_{dl}. R_s and C_s are not frequency independent, but are less so than R_p and C_p, so that the equivalent circuit of Fig. 2a is clearly a better approximation to the cell circuit than a parallel R_p, C_p combination.

A more realistic representation [2,4,5] of the equivalent cell circuit is shown in Fig. 6. $R_W(\omega) + C_W(\omega)$ are the resistive and capacitive components of the so-called Warburg impedance, which arises from concentration polarization due to electrode reactions, and R_F is the so-called Faradaic impedance associated with the electrode reaction itself. In Fig. 6 we have neglected capacitance between the conductivity cell leads and capacitance due to the dielectric constant of the electrolyte, since these contribute a negligible amount to the audio frequency impedance of the low impedance cell under consideration.[2]

Equivalent circuit analysis of Fig. 6 (Appendix 1) gives for the equivalent series resistance:

$$R_s = R_L + R_{sol} + \frac{\left\{\left[R_F + R_W(\omega)\right]^2 + \left[1/\omega C_W(\omega)\right]^2\right\}\left[R_F + R_W(\omega)\right]}{\left[R_F + R_W(\omega)\right]^2 + \left\{\omega C_{dl}\left[\left(R_F + R_W(\omega)\right)^2 + (1/\omega C_W(\omega))^2\right] + (1/\omega C_W(\omega))\right\}^2} \tag{10}$$

Both $R_W(\omega)$ and $(1/\omega C_W(\omega))$ are frequency dependent with an $\omega^{-1/2}$ dependence,[4] so that the high frequency limit of R_s is

$$\lim_{\omega \to \infty} R_s = R_L + R_{sol} \tag{11}$$

Equivalent circuit analysis of Fig. 6 shows that R_p approaches an identical high frequency limit, but at a slower rate (compare Eq. (2)).

4. G. J. Hills and S. Dordjevic, Electrochim. Acta, 13, 1721 (1968).
5. G. D. Robbins, J. Electrochem, Soc., 116, 813 (1969).

The data of Figs. 4 and 5 exhibit this predicted behavior, that is

(a) both R_s and R_p converge to the same limiting values at high frequencies, R_s more quickly than R_p;

(b) the resistance values for both platinized and unplatinized electrodes converge to the same high frequency limit.

The electrode impedances for the platinized electrodes are such that R_s and R_p converge at lower frequencies than for the unplatinized electrodes, so that we may take the limiting high frequency value of R_s = 0.261 Ω for the platinized electrodes and identify it with $(R_L + R_{sol})$. This agrees within experimental error with the value of $(R_L + R_{sol})$ = 0.256 Ω calculated from the independently measured values of R_L, (L/A), and K_{sol} for the 45% of KOH solution:

$$(R_L + R_{sol}) = R_L + (L/A)/K_{sol} \tag{12}$$

CONCLUSIONS

We have shown here that one may obtain correct measurements of $(R_L + R_{sol})$ and hence also obtain correct measurements of $(R_L + R_{sol} + R_{sep})$ and therefore of R_{sep} by audio frequency ac bridge measurements on low impedance conductivity cells if some precautions are observed. In particular, since even with platinized electrodes (cf. Fig. 5) R_p and R_s reach their limiting high frequency values only at the higher frequency end of the audio range, it is plainly not sufficient to make a measurement of R_p at a single frequency and assume it equal to $(R_L + R_{sol})$ or $(R_L + R_{sol} + R_{sep})$. Rather it is recommended that for low impedance cells R_p and C_p measurements be made as a function of frequency, that R_s be calculated from R_p and C_p via Eq. 8, and that the limiting high frequency value of R_s be identified with $(R_L + R_{sol})$ or $(R_L + R_{sol} + R_{sep})$. Heavily platinized electrodes should be used, since these lead to convergence of R_s to its limiting value within the observable frequency range (Fig. 5), while unplatinized electrodes may require extrapolation of R_s beyond the audio range in order to obtain the high frequency limit.

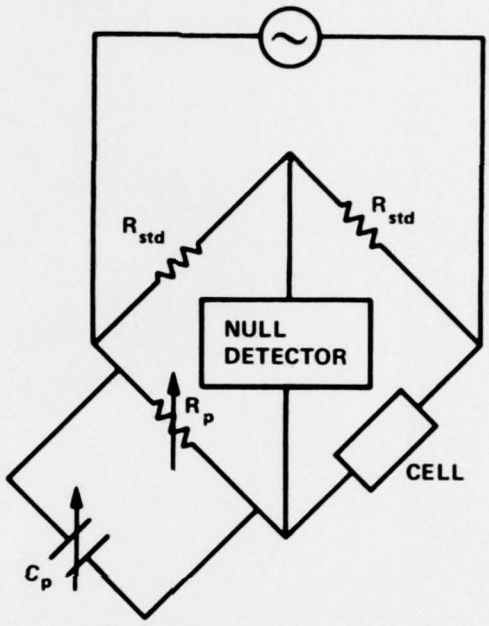

FIG. 1 A. C. WHEATSTONE BRIDGE FOR MEASURING EQUIVALENT PARALLEL RESISTANCE R_p AND CAPACITANCE C_p OF CONDUCTIVITY CELL.

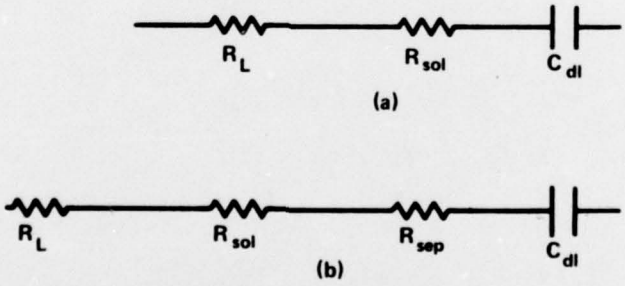

FIG. 2 APPROXIMATE EQUIVALENT CIRCUITS OF CONDUCTIVITY CELL CONTAINING (a) ELECTROLYTE SOLUTION AND (b) ELECTROLYTE SOLUTION PLUS SEPARATOR.

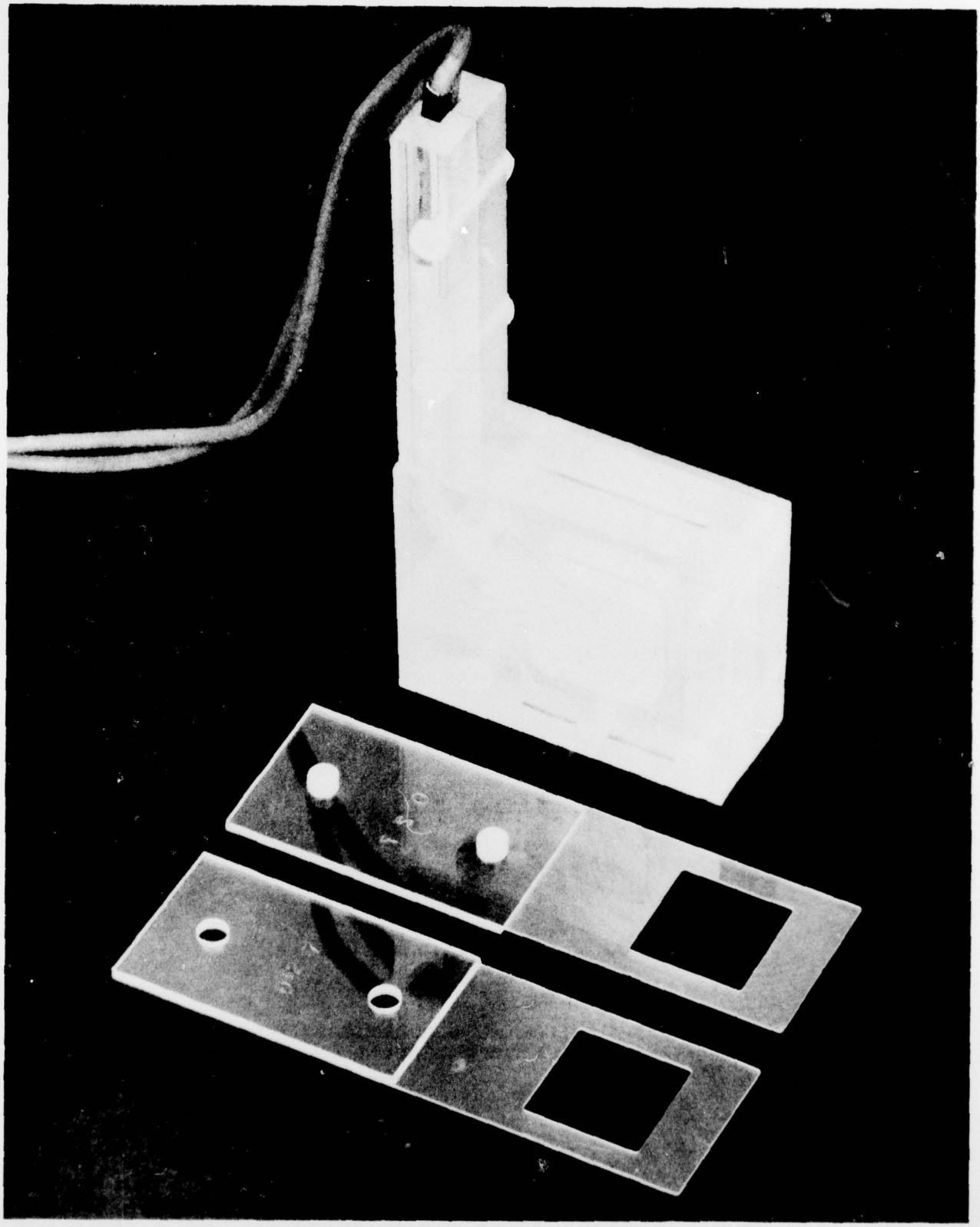

FIG. 3 CONDUCTIVITY CELL FOR MEASUREMENT OF MEMBRANE RESISTANCES.

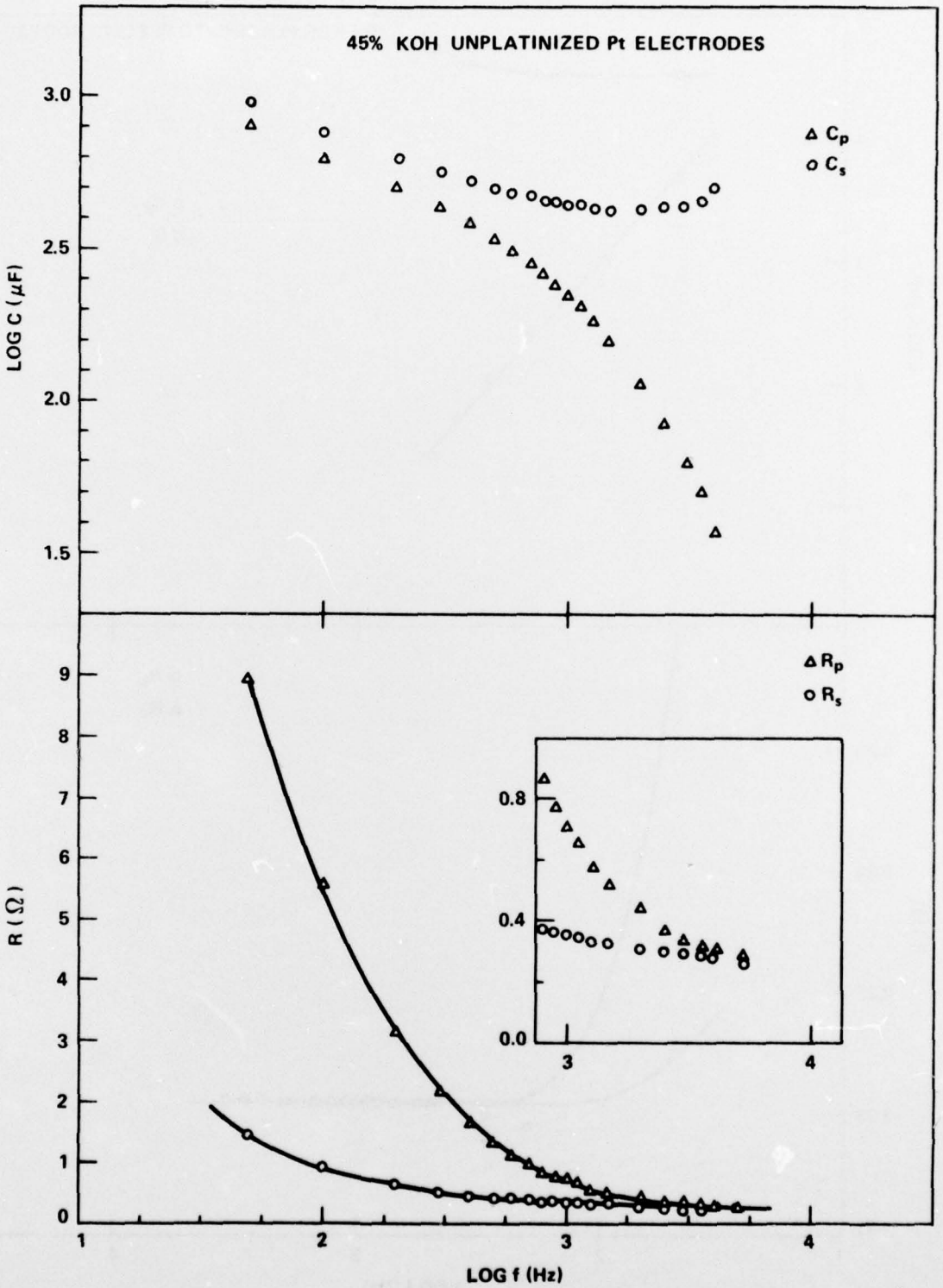

FIG. 4 EQUIVALENT PARALLEL AND SERIES RESISTANCES AND CAPACITANCES VERSUS FREQUENCY OF A CONDUCTIVITY CELL FILLED WITH 45% KOH SOLUTION AT 25.0° C USING UNPLATINIZED Pt ELECTRODES. INSERT IS AN ENLARGED PLOT OF THE DATA AT HIGH FREQUENCY.

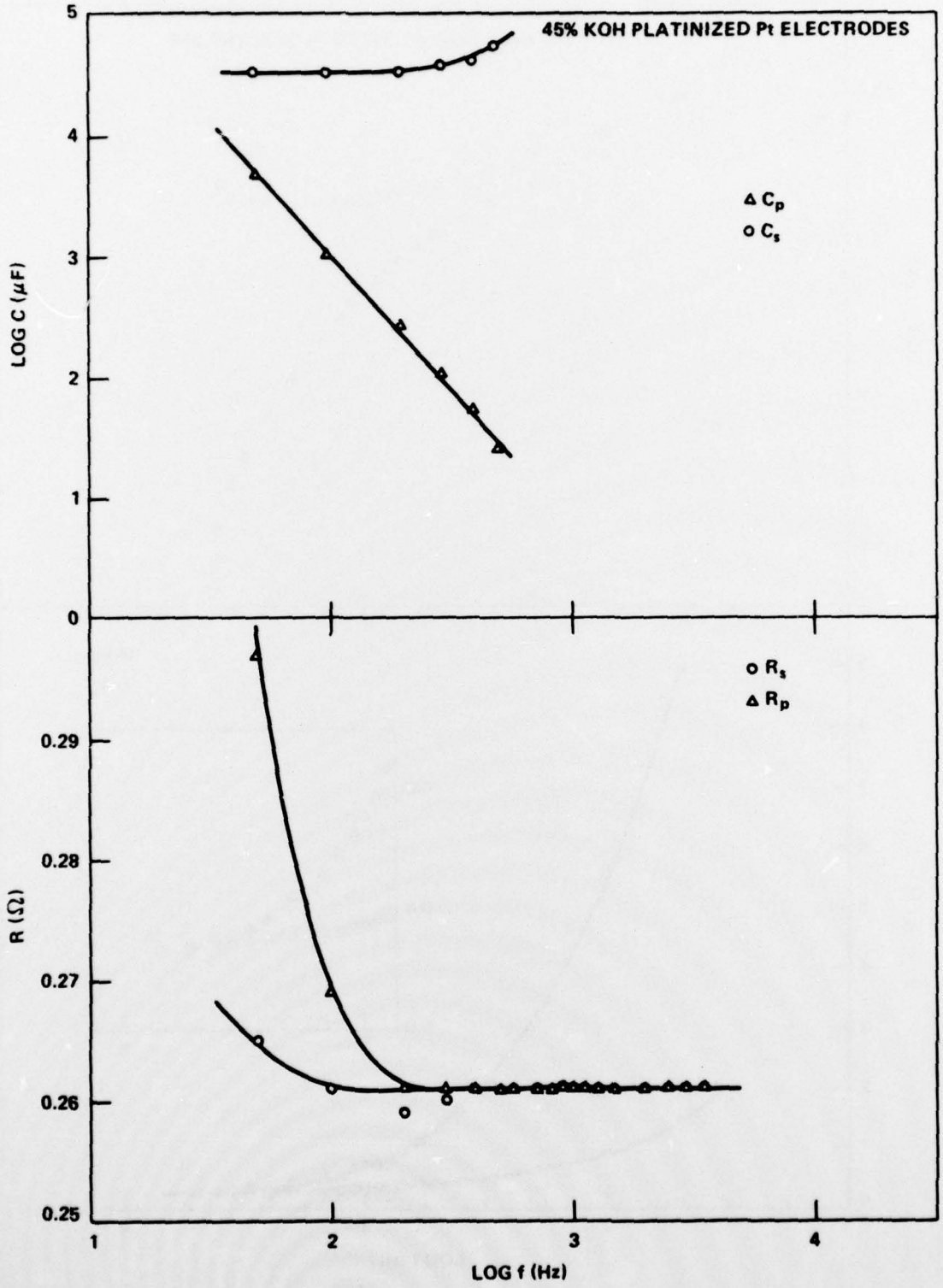

FIG. 5 EQUIVALENT PARALLEL AND SERIES RESISTANCES AND CAPACITANCES VERSUS FREQUENCY OF CONDUCTIVITY CELL FILLED WITH 45% KOH SOLUTION AT 25.0° C USING PLATINIZED Pt ELECTRODES.

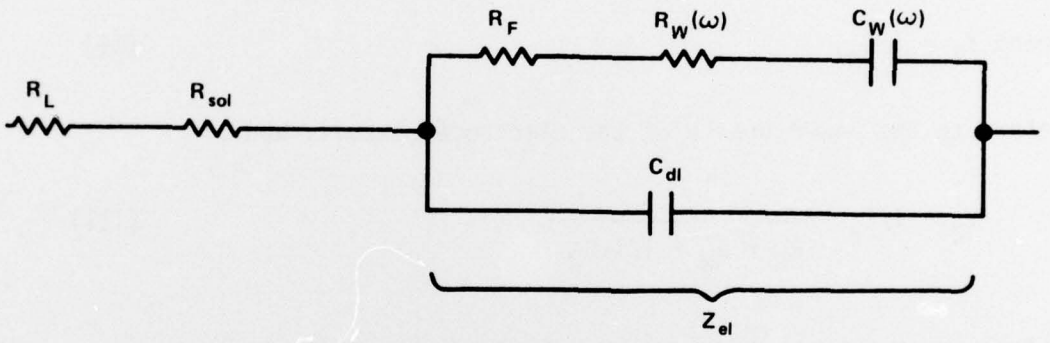

FIG. 6 EQUIVALENT CIRCUIT OF CONDUCTIVITY CELL CONTAINING ELECTROLYTE.

APPENDIX 1

Equivalent Circuit Analysis of Fig. 6.

$$Z = R_L + R_{sol} + Z_{el} = R_L + R_{sol} + 1/Y_{el}$$

$$= R_L + R_{sol} + 1/(Y_1 + Y_2) \qquad \text{(I)}$$

where $Y_1 = i\omega C_{dl}$ (II)

refers to the lower branch of the electrode circuit, and

$$Y_2 = 1/Z_2 = \frac{1}{R_F + R_W + 1/i\omega C_W} \qquad \text{(III)}$$

refers to the upper branch of the electrode circuit.

Substituting equations (II) and (III) into equation (I) and taking the real part gives Eq. (10):

$$R_s = Re\ (Z)$$

DISTRIBUTION

NAME	COPIES
Naval Sea Systems Command Washington, D. C. 20362	
Attention: Code SEA 09G32	2
Code SEA 03B	1
Code SEA 0331J (S. J. Matesky)	1
Code SEA 0331 (J. W. Murrin)	1
Code SEA 0841B (J. R. Cipriano)	1
Office of Naval Research Washington, D. C. 20360	
Attention: Library	1
Office of Naval Research 800 N Quincy Street Arlington, VA 22217	
Attention: Code 472 (Dr. G. A. Neece)	1
Naval Research Laboratory Washington, D. C. 20390	
Attention: Code 6170 (A. C. Simon)	1
Defense Nuclear Agency Washington, D. C. 20301	
Attention: Library	1
Headquarters, USAFSS Airforce Special Communications Center San Antonio, TX 78243	
Attention: Library	1
Defense Documentation Center Cameron Station Alexandria, VA 22314	
Attention: Library	12

Headquarters, US Army Development & Readiness Command
5001 Eisenhower Avenue
Alexandria, VA 22333
Attention: Code DRCDE-L (J. W. Crellin) 1

US Army Electronics Command
Fort Monmouth, NJ 07703
Attention: Code DRSEL-TL-P (D. Linden) 1
Code DRSEL-TL-PR (Dr. S. Gilman) 1

Naval Weapons Center
China Lake, CA 93555
Attention: Dr. Aaron Fletcher 1

US Army Mobility Equipment R & D Command, Electrochemical Div
Fort Belvoir, VA 22060
Attention: Code DRDME-EC 1

Naval Ship Engineering Center
Washington, D. C. 20362
Attention: Code 6157D (A. Himy) 1

Naval Intelligence Support Center
4301 Suitland Road
Washington, D. C. 20390
Attention: Code 362 (Dr. H. E. Ruskie) 1

Naval Material Command
Washington, D. C. 20360
Attention: Code NAVMAT 0323 (I. Jaffe) 1
Code NAVMAT 03533 (R. H. Abrams) 1

National Aeronautics and Space Administration
Washington, D. C. 20546
Attention: Library 1

Naval Undersea Center
San Diego, CA 92132
Attention: Library 1

EIC Corporation
55 Chapel Street
Newton, MA 02158
Attention: J. R. Driscoll 1

Edgewood Arsenal
Aberdeen Proving Ground, MD 21010
Attention: Library 1

AF Aero Propulsion Lab
Wright-Patterson AFB, OH 45433
Attention: Code AFAPL/POE-1 (W. S. Bishop) 1
Code AFAPL/POE-1 (J. Lander) 1

NASA Goddard Space Flight Center
Greenbelt, MD 20771
Attention: Code 711 (G. Halpert) 1

NASA Lewis Research Center
21000 Brookpark Road
Cleveland, OH 44135
Attention: Code MS 309/1 (Dr. J. S. Fordyce) 1

Frank J. Seiler Research Laboratory
AFSC, USAF Academy, CO 80840
Attention: Code FJSRL/NC (Capt. J. K. Erbacher, USAF) 1

Naval Weapons Support Center
Electrochemical Power Sources Division
Crane, IN 47522
Attention: Code 305 (D. G. Miley) 1

Energy Research & Development Administration
Division of Electric Energy Systems
Room 2101
Washington, D. C. 20545
Attention: L. J. Rogers 1

Energy Research & Development Administration
Division of Applied Technology
Washington, D. C. 20545
Attention: Code M/S E-463 (Dr. A. Langrebe) 1

Strategic Systems Project Office
Engineering Development Project Office
Washington, D. C. 20360
Attention: Code NSP-2721 (K. N.Boyley) 1

Nuclepore Corporation
7035 Commerce Circle
Pleasanton, CA 94566
Attention: Dr. M. C. Porter 1

Naval Underwater Systems Center
Newport, Rhode Island 02840
Attention: Code 3642 (T. Black) 1

Union Carbide, Nuclepore Corporation
7035 Commerce Circle
Pleasantown, CA 94566
Attention: Library 1

Naval Air Systems Command
Department of the Navy
Washington, D. C. 20361
Attention: Code NAVAIR 310C (Dr. H. Rosenwasser) 1

Harry Diamond Lab
Chief, Power Supply Branch
2800 Powder Mill Road
Adelphi, MD 20783
Attention: Code DRXDO-RDD (A. A. Benderly) 1

Catholic University
Chemical Engineering Department
Washington, D. C. 20064
Attention: Dr. C. T. Moynihan) 1

David W. Taylor Naval Ship R & D Ctr.
Annapolis Laboratory
Annapolis, MD 21402
Attention: Code 2723 (A. B. Neild) 1
Code 2724 (J. Woerner) 1

Naval Electronics Systems Command
Washington, D. C. 20360
Attention: Code PME 124-31 (A. H. Sobel) 1

John Hopkins Applied Physics Lab
John Hopkins Road
Laurel, MD 20810
Attention: Library 1

Catalyst Research Corp.
1421 Clarkview Road
Baltimore, MD 21209
Attention: George Bowser 1

Headquarters, Dept. of Transportation
US Coast Guard, Ocean Engineering Division
Washington, D. C. 20590
Attention: Code GEOE-3/61 (R. Potter) 1

RAI Corporation
225 Marcus Blvd.
Hauppauge, New York 11787
Attention: Vincent F. D'Agostino

Catholic University of America
620 Michigan Avenue
Washington, D. C. N. E. 20017
Attention: Dr. C. T. Moynihan